

Review

Recent Advance on Polyaniline or Polypyrrole-Derived Electrocatalysts for Oxygen Reduction Reaction

Zhankun Jiang *, Jiemei Yu, Taizhong Huang and Min Sun *

School of Chemistry and Chemical Engineering, University of Jinan, 336 West Nanxinzhuang Road, Jinan 250022, China; chm_yujm@ujn.edu.cn (J.Y.); chm_huangtz@ujn.edu.cn (T.H.)

* Correspondence: zhankun.jiang@emt.inrs.ca (Z.J.); chm_sunm@ujn.edu.cn (M.S.)

Received: 15 October 2018; Accepted: 6 December 2018; Published: 17 December 2018



Abstract: The fuel cell, as one of the most promising electrochemical devices, is sustainable, clean, and environmentally benign. The sluggish oxygen reduction reaction (ORR) is an important fuel cell cathodic reaction that decides the efficiency of the overall energy conversion. In order to improve ORR efficiency, many efficient catalysts have been developed, in which the *N*-doped material is most popular. Polyaniline and polypyrrole as common aromatic polymers containing nitrogen were widely applied in the *N*-doped material. The shape-controlled *N*-doped carbon material can be prepared from the pyrolysis of the polyaniline or polypyrrole, which is effective to catalyze the ORR. This review is focused on the recent advance of polyaniline or polypyrrole-based ORR electrocatalysts.

Keywords: oxygen reduction reaction; fuel cell; polyaniline; polypyrrole; *N*-doped carbon

1. Introduction

A fuel cell is a device that directly transfers chemical energy stored in fuel and oxidizer to electrical energy [1–3]. It is different from conventional batteries in that the fuel cell generates electricity as long as the fuel is continuously supplied. Because it is not restricted by the Carnot cycle, the energy conversion efficiency can reach 40–60%, 1.5–2 times that of the internal combustion engine, it is also environmentally friendly (emissions of CO₂ or water) and produces no noise. Therefore, it is considered to be the most promising clean and efficient power generation technology. One major hindrance of fuel cell application is the sluggish oxygen reduction reaction (ORR) [4–6]. The reaction occurs on the cathode as a half reaction. The commercial Pt/C catalysts are the most applied catalysts [7–9]. However, platinum is rare and very expensive. In addition, Pt particles may be peeled off or aggregate in the catalysis process, which causes a decrease in activity [10–13]. Therefore, the development of efficient ORR catalysts is one of the most important factors for the fuel cell.

In order to replace Pt/C, three types of electrocatalysts are mainly researched, including non-metal catalysts [14,15], non-noble metal catalysts [16–19], and low-content noble metal catalysts [20,21]. Carbon materials, as the essential support of electrocatalysts, were usually doped by a heteroatom (N, B, P, S, etc.) [22–26] to improve the activity of ORR electrocatalysts. The nitrogen-doped carbons are the most promising catalyst materials for ORR [27–29]. Two types of aromatic polymers including polyaniline (PANI) and polypyrrole (PPy) are used to provide nitrogen atoms and control the morphology.

PANI and PPy are both widely used conductive polymers [30–32]. Their morphology can be controlled with different synthesis methods. After pyrolysis, the morphology-controlled nitrogen doping carbon can be obtained. Furthermore, the nitrogen content of the polymer derived *N*-doped carbon is also controllable. This mini-review focuses on PPy- and PANI-derived electrocatalysts for

the oxygen reduction reaction (ORR). Because the two main challenges in the ORR catalysts design are high efficiency and stability, many PANI- and PPy-derived materials have been designed. This review presents the representative works and suggests potential prospective researches.

2. Polyaniline-Derived Catalysts for Oxygen Reduction Reaction

In order to get efficient ORR catalysts, metal-free materials, noble metal-free materials, and noble metal materials are normally used. The noble metal sticks to the Pt and Pt alloys. Polyaniline-derived catalysts are efficient for ORR.

2.1. Metal-Free Polyaniline-Based Catalysts

N-doped carbon, which is one of the most promising ORR catalysts, can be obtained through the pyrolysis of PANI-based materials. The effect of nitrogen is still under study. The N species contain pyridinic-, pyrrolic-, and graphitic-nitrogen. Pyridinic N possesses better activity than graphitic N because of their different sp^2 electronic structures [33]. For the metal-free PANI-based ORR catalysts, researchers make many efforts to control the morphology of the catalysts. The PANI nanotubes were pyrolyzed at different temperatures. After pyrolysis, the morphology of the nanotubes was maintained and typical nitrogen species, such as pyrrolic-, pyridinic-, and graphitic-N, were obtained. The product fabricated at 700 °C (NCNT-700) exhibited the highest electrocatalytic ORR activity, long-standing stability, and good tolerance against methanol. The half-wave potential of the NCNT-700 is 0.84 V vs. RHE. The improved activity is mainly attributed to the high nitrogen level of the active pyridinic and graphitic N. JingJing Xu et al. [34] developed a highly efficient ORR catalyst derived from PANI@CNTs-sulfonated polystyrene. Quilez-Bermejo Javier et al. [35] studied the activity of N-doped carbons derived from PANI. When the pyrolysis was processed at a high temperature above 1100 °C, the conversion from pyridine to quaternary N in the edge position occurred and resulted in excellent ORR activity. The catalysts derived from PANI nanofiber and glucose showed high onset potential (−0.171 V vs. Ag/AgCl), large limiting current density, and a 4-electron process [36]. Perchloric acid ($HClO_4$) was used as an oxidant and pore-forming agent in an electrochemical polymerization [37]. In the first step, carbon paper was used in a traditional three-electrode system. $HClO_4$ and aniline were used as the electrolyte solution. Secondly, the materials were carbonized under a nitrogen atmosphere. The obtained material shows a high surface area of $1341.12 \text{ m}^2 \text{ g}^{-1}$ and high N content. PANI-derived mesoporous carbon was obtained based on yolk-shell nanostructured polyaniline@ SiO_2 particles [38], and the SiO_2 particles were used as the hard template. The electrocatalyst presented high stability and tolerance to CH_3OH . B/N [39] and N,P [40] co-doped carbon materials were developed and showed high ORR activity. Quilez-Bermejo Javier et al. [41] heated the PANI and de-doped PANI (PANId) under two different atmospheres: a pure inert atmosphere (N_2) and a slightly oxidizing mixture of gases (3000 ppm O_2 in N_2). Interestingly, the pyrolysis under 800 °C using a slight oxidant atmosphere produces carbon materials with much higher ORR activity. The authors believe the larger amount of N-edge and O-edge sites contribute to the phenomenon. Therefore, in the pyrolysis process, the commonly used inert atmosphere may not be the best choice.

2.2. Noble Metal-Free Polyaniline-Based Catalysts

Some nonprecious metals, represented by iron, cobalt, nickel, and manganese, were used to generate the efficient ORR electrocatalysts. Among the non-noble metal-based ORR catalysts, Fe-N-C is one of the most promising materials [42–45]. Compared to commercial Pt/C, Fe-N-C has several advantages such as low price, high efficiency, tolerance to the toxicity of CO, and long life.

Gang Wu et al. [46] incorporated iron and/or cobalt in the PANI-derived carbon catalyst. Firstly, aniline oligomer was mixed with carbon particles and transition metal precursors (cobalt nitrate and/or iron chloride), followed by the addition of ammonium persulfate as an oxidant to fully polymerize the aniline. After the polymerization process, the materials underwent pyrolysis in an N_2 atmosphere. Among the prepared materials, PANI-Fe-C and PANI-FeCo-C materials showed

similar ORR activity, and the half potential of the materials was slightly lower than that of Pt/C. The mechanism study showed a four-electron process, and the hydrogen peroxide yield was smaller than 1.0%. The PANI-derived catalysts showed high durability according to the fuel-cell performance test as well as the RDE test.

In order to insight the active sites of Fe-N-C catalyst, PANI and cyanamide were used as nitrogen precursors [16]. The prepared materials showed much larger micropore surface area and the volumes of mesopores (pore diameter 2 to 50 nm) was $\sim 0.25 \text{ cm}^3 \text{ g}^{-1}$. The authors concluded that the edge-hosted FeN_4 sites contribute to the high activity in the Fe-N-C catalyst. Researchers found that a pore width between 5 and 20 angstroms [47] had a great influence on activity. The prepared material has a large mesopore surface area. When the precursor is PANI alone, the Brunauer–Emmett–Teller (BET) surface area is nearly $1000 \text{ m}^2 \text{ g}^{-1}$, and when the precursor is PANI and CM, the surface area is nearly $1600 \text{ m}^2 \text{ g}^{-1}$. The prepared catalysts processed a four-electron pathway, and the yield of hydrogen peroxide was lower than 2%. Carbon-embedded nitrogen-coordinated iron (FeN_4) was proposed as the catalytic active site. Aberration-corrected scanning transmission electron microscopy was used to visualize the FeN_4 site, and the contributions of these active sites associated with specific lattice-level carbon structures were explored computationally.

Yang Hu et al. [48] used PANI nanofibers as nitrogen and carbon precursors. The mass content of Fe was 0, 0.3, 0.5, 1.0, 3.0, 5.0, and 10.0 wt %. The 3.0 Fe-PANI catalyst showed the best onset potential: 0.905 V vs. RHE. The materials process a four-electron ORR pathway. Prussian blue analogue (PBA, $\text{Co}_3[\text{Fe}(\text{CN})_6]_2$) and polyaniline (PANI) were mixed as the precursor [49]. The 2–5 nm PBA nanocrystals homogeneously dispersed in PANI. The PBA nanocrystals are the precursor for the active sites, and are also the template for pore formation in the pyrolysis process. The catalysts exhibit ORR activity comparable to that of the commercial Pt/C (20 wt % Pt loading) in the alkaline and acidic environment. Carbon nanotubes (CNTs) were used to support Fe-PANI [50]. Jian Zhang et al. [51] pyrolyzed the polyaniline on carbon nanospheres, and ferric chloride was used as an oxidant and iron source. The scheme is shown in Figure 1. The authors concluded that the as-prepared catalyst shows a high activity and much better stability than that of commercial Pt/C in an acid medium. Guanghua Wang et al. [52] prepared an N-doped carbon catalyst with trace iron (0.54 wt. % Fe). The PANI-iron coordination polymers were pyrolyzed.

Other nonprecious metals, such as cobalt, nickel, and manganese, were also used to generate electrocatalysts for ORR. Shiyi Cao et al. [53] synthesized mesoporous hybrid shells of carbonized polyaniline (C-PANI)/ Mn_2O_3 . The manganese oxide hybrid materials showed high ORR electrocatalytic activity. In particular, the onset potential is +0.974 V (versus RHE), the specific current is 60.8 mA/mg, and the electronic transfer number is 4. The remarkably high ORR activity can be attributed to the high specific surface area, the surface oxidation state of Mn, and composition-codependent behavior. PANI and beta- MnO_2 nanocomposites [54] were also built. PANI nanofibers were hybridized with cobalt nitrate [55]. After pyrolysis, the PANI nanofibers formed graphene networks with N-doped. It is a facile and scalable approach to the synthesis of Co and N codoped graphene networks for ORR in acidic solutions with high activity and excellent durability. Furthermore, the NiCo-doped PANI precursors underwent pyrolysis in an inert atmosphere at $800 \text{ }^\circ\text{C}$ [56], and the molar ratio of Ni and Co was adjusted. Among the prepared catalysts, the catalyst $\text{Ni}_6\text{Co}_1/\text{C-N}$, which showed the largest surface area according to the BET method, presented the best ORR activity and stability. PANI was used to reduce Ag^+ cations [57] to get catalysts. The Ag dendrites were readily generated in PANI nanofiber dispersion via the redox reaction between AgNO_3 and PANI.

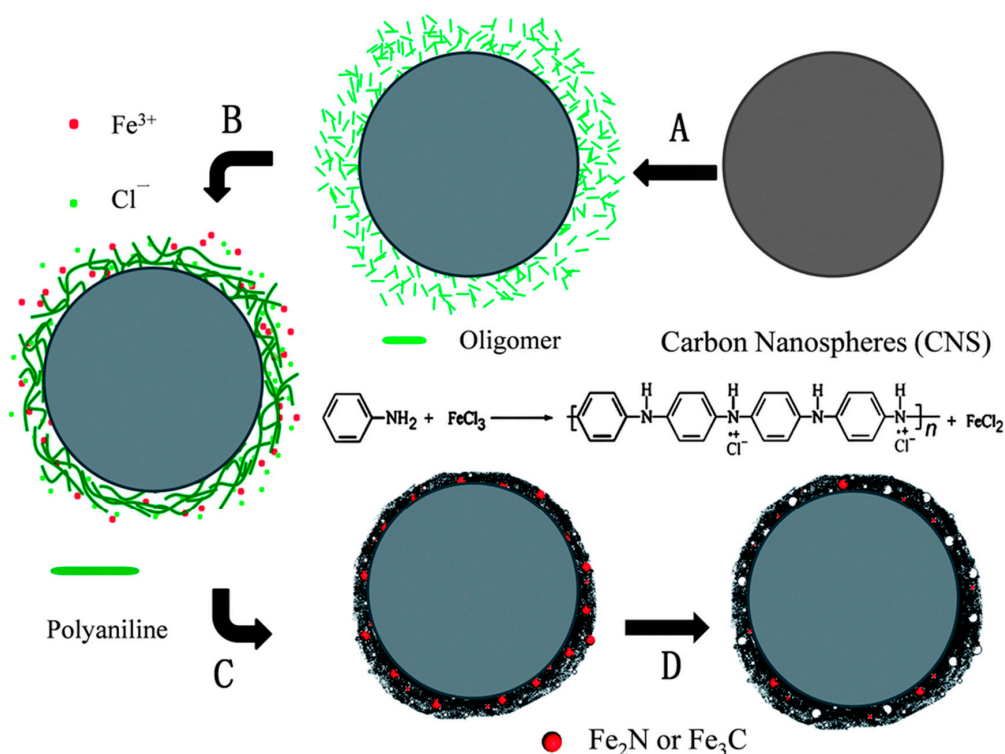


Figure 1. Schematic of the synthesis process of the $\text{FeN}_x\text{C}/\text{C}-\text{F}$ catalyst [51]. (A) Mixing of CNS with aniline oligomers. (B) Oxidative polymerization of aniline by addition of FeCl_3 solution. (C) First heat treatment in an ammonia atmosphere. (D) Acid leaching. The second heat treatment after acid leaching is not shown.

2.3. Noble Metal Polyaniline-Based Catalysts

In the harsh chemical and electrochemical conditions, the carbon supports are susceptible to corrosion. In order to increase the stability, which is the key factor in catalyst application, PANI was used as a protector to inhibit carbon nanospheres from corrosion of the carbon supports. In order to improve the durability of the Pt-based ORR catalysts, perfluorosulfonic acid (PFSA) and PANI were used to co-stabilize Pt catalysts [58]. The prepared Pt-PFSA/C@PANI catalyst shows comparable activity with the commercial Pt/C. Furthermore, the catalyst shows much higher stability than the commercial Pt/C. The stability is very important for this Pt-based catalyst. The stability can be concluded to the result of PFSA and PANI. The Pt NPs were wrapped by PFSA (Pt@PFSA). Then the Pt@PFSA were anchored on C@PANI. The coating of PANI on carbon supports can cover the surface of the carbon supports, and this causes the micropores on the surface of the carbon to disappear. The phenomenon can prevent Pt NPs being embedded in the micropores. The dual PFSA and PANI polymers are important for the stability of the as-prepared catalyst.

The Pt-based alloy is also used to enhance the ORR activity and reduce the Pt content [59]. Yang Liu et al. [60] prepared several Pt-Co/C-PANI catalysts via a microwave-assisted polyol method. The best-prepared catalysts showed a mass activity of $1.33 \text{ A mg}_{\text{Pt}}^{-1}$ and specific activity of 1.29 mA cm^{-2} , and the performance was 7.8 and 5.4 times higher than that of Pt/C catalyst. The ORR activity and stability of Pt and PtM (M = Ni, Co, Cr, Pd) supported on polyaniline/CNTs were explored and compared with the commercial Pt/C catalyst [61].

3. Polypyrrole-Derived Catalysts for Oxygen Reduction Reaction

Like the PANI-derived catalysts, the polypyrrole-derived catalysts can also be divided into 3 kinds: metal-free, noble metal-free, and noble metal.

3.1. Metal-Free Polypyrrole-Derived Catalysts

Hongli An et al. [62] polymerized PPy in a CNT matrix, then the CNTs were covered with PPy on the surface (CNTs@PPy). Then the hybrid material underwent pyrolysis to obtain an N-doped CNT. The ORR activity is shown in Figure 2. The as-obtained NCNTs exhibited an onset potential of 0.95 V, a diffusion-limited current of 6.82 mA cm^{-2} , and excellent stability in alkaline media. The results indicate that the high ORR performances were mainly derived from the pyridinic-N in the NCNTs. Furthermore, the ratio of three different nitrogens (pyridinic, pyrrolic, or graphitic N) can be easily tuned by adjusting the amount of PPy in the CNTs@PPy core-shell precursors.

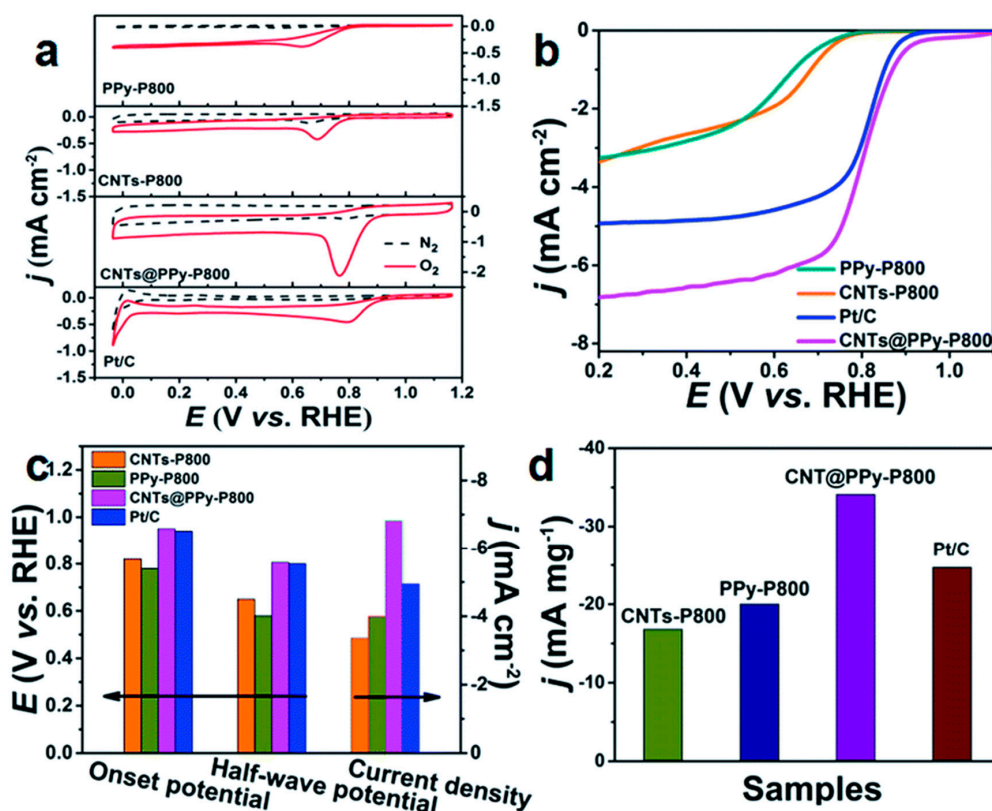


Figure 2. (a) CV curves of PPy-P800, CNTs-P800, CNTs@PPy-P800, and Pt/C in N₂ and O₂-saturated solution, respectively. (b) LSV curves of PPy-P800, CNTs-P800, CNTs@PPy-P800, and Pt/C catalyst in O₂-saturated 0.1 M KOH solution at a sweep rate of 10 mV s^{-1} and an electrode rotation speed of 1600 rpm . (c) The onset potential, half-wave potential, and current density of PPy-P800, CNTs-P800, CNTs@PPy-P800, and Pt/C, respectively. (d) Corresponding mass activities of these four samples [62].

In order to improve the activity and lifetime of the catalysts, other heteroatoms such as P, S, and F were also added. Phytic acid was used as P-dopant, and polystyrene sphere was used as a template [63]. After the pyrolysis process, the resultant N,P-MC materials exhibited spherical mesopores with an average diameter of ca. 70 nm. The BET surface area of the N,P-MC sample is $305 \text{ m}^2 \text{ g}^{-1}$. N,P-MC exhibits best ORR activity among the prepared materials. The material performs a 4-electron process, has high ORR activity, and good methanol tolerance. The mesoporous structure, high surface area, and increased active sites (N,P) are key factors that improve ORR performance. Researchers [64] synthesized nitrogen-doped carbon nanofiber films (NCNFs) via the carbonization of polypyrrole-functionalized electrospun polyacrylonitrile (PAN) nanofibers. A triazine-based polypyrrole network (TPN) was synthesized and then pyrolyzed to get an N-rich carbon catalyst [65]. In the TPN synthesis process, the 2,4,6-tripyrrol-1,3,5-triazine monomer was used; the protonating agent was TfOH and the oxidizing agent was benzoyl peroxide. The obtained NC-900 (pyrolyzed at $900 \text{ }^\circ\text{C}$) catalyst, which presents a surface area of $779 \text{ m}^2 \text{ g}^{-1}$ and contains 3.02% nitrogen, exhibits

promising ORR activity in alkaline media. Two key ORR parameters—onset potential and half-wave potential of prepared NC-900—are both higher than those of Pt/c. Furthermore, the as-prepared material shows better MeOH tolerance and higher durability.

The relationship between the morphology of PPy and the corresponding ORR activity were studied [66]. The granular- and tubules-like PPy was annealed at 800 °C with morphology maintained. For the ORR catalyst performance, such as onset potential, half-wave potential, electron number, and stability, the tubules-like carbon was better than the granular-like carbon. The higher catalytic activity was explained by a better electrical conductivity in the tubular structure than in the granular one.

3.2. Non-Noble Metal Polypyrrole-Derived Catalysts

A series of Fe-N-C electrocatalysts derived from PPy were designed and studied [67]. In the catalysis preparation, mesoporous carbon (MPC), PPy, and Fe(II) acetate were used as the C source, N source, and Fe source, respectively. Firstly, polyvinylpyrrolidone (PVP) was added to a MPC-PPy support, and the hybrid material was heat-treated. Secondly, the pyrolysis carbon support was further impregnated with Fe²⁺ ions. The authors concluded that the microporosity of the prepared catalysts directly influences the ORR activity. The same research team [68] synthesized a Fe-Co-N-C catalyst for ORR according to a sacrificial method. Also, pyrrole was used as an inexpensive precursor for N-doped carbon materials. Alkaline membrane fuel cells (AMFC) were used in the research. A high performance for AMFC, 420 mW cm⁻² at 60 °C, was achieved. Furthermore, a good performance of alkaline direct ethanol fuel cells was achieved. Min Sun et al. [69] use electrochemical polymerization method to synthesize structured Fe-N-C ANFs/CP (activated NFs derived from PPy doped with iron atoms in situ grown on carbon paper) on a carbon paper. The authors focused on the connection between iron concentration and ORR activity. The research showed that the 0.05-Fe-N-C ANFs exhibited the highest activity and good durability. The high activity is ascribed to the high Fe-N_x concentration, the porous structure, and well-dispersed active sites.

A novel kind of tetrazine-based polypyrrole spheres (PTPys) was prepared by protonic acid catalyzed Friedel–Crafts polymerization of bis(*N*-pyrrolyl)-1,2,4,5-tetrazine (TPy) with dimethoxymethane in dichloroethane [70]. Firstly, PTPys with a diameter of 100 to 300 nm were synthesized and pyrolyzed at 900 °C to generate N-doped porous carbon spheres (N/Cs-900 electrocatalyst). Then Fe(OAc)₂ were mixed with PTPys and then pyrolysis to get N/Fe-codoped porous carbon spheres (Fe/N-Cs-900 electrocatalyst). The Fe/N-Cs-900 catalyst showed the best ORR activities. In the acidic solution, the Fe/N-Cs-900 catalyst exhibited excellent activity, which is comparable to the Pt/C catalyst. In the alkaline solution, the Fe/N-Cs-900 catalyst showed better ORR performance than Pt/C. The well-defined spherical architecture, high N content, high surface area, and porosity contributed to the high ORR activities. Haodong Sha et al. [71] experimentally studied the active sites for ORR catalysts. A series of carbon-supported cobalt-polypyrrole-4-toluenesulfonic acids were pyrolyzed in an inert atmosphere at 800 °C, then electrochemically evaluated in aqueous 0.5 M sulfuric acid. A series of catalysts were prepared. Metallic cobalt, cobalt oxide, and nitrogen species (Co-N_x) bonded to cobalt were formed. Co-N_x, which is the active site, was formed when the cobalt loading was less than 1.0 wt %. When the loading was higher than 1.0 wt %, metallic Co and Co oxide particles coexisted with the Co-N_x compound. Both metallic Co and Co oxide were not active for catalyzing ORR. As a result, at a Co loading of ~1.0 wt %, the catalyst gave the best ORR activity. The ORR active site in (Co-PPy-TsOH/C)_P catalyst was likely a Co-pyridinic-N group. A ternary CoNiMn-layered double hydroxide (LDH)/PPy/reduced graphene oxide (rGO) composite was fabricated by one-step involving the formation of the LDH and polymerization of the pyrrole (Py) [72].

Non-noble metal oxides were also studied. A novel strategy based on block copolymer self-assembly in solution were developed recently [73]. The prepared materials were two-dimensional graphene-based mesoporous nanohybrids with well-defined large pores of tunable sizes. In the process, polystyrene-block-poly (ethylene oxide) spherical micelles were used as the pore-creating template.

The PPy monolayers were grown on both sides of rGO nanosheets, and Fe₂O₃ NPs were embedded in them (denoted as mPPy-Fe₂O₃@rGO). Furthermore, the materials were heated at 800 °C to get sandwich-like mesoporous nitrogen-doped carbon/Fe₃O₄/rGO (mNC-Fe₃O₄@rGO). The prepared mNC-Fe₃O₄@rGO materials show excellent electrocatalytic activity with a four-electron transfer nature, a high half-wave-potential of +0.84 V, and a limiting current density of 5.7 mA cm⁻². Co₃O₄ nanoparticles were assembled on a polypyrrole/graphene oxide electrocatalyst ((CoO₄)-O-3/PPy/GO) as an efficient catalyst for the oxygen reduction reaction (ORR) in alkaline media [74]. By one-step in situ ball milling of graphite, pyrrole, and cobalt salt without resorting to high-temperature annealing, a facile strategy was developed to synthesize cobalt oxide and PPy coupled with a graphene nanosheet (Co₃O₄-PPy/GN) complex [75]. The as-prepared Co₃O₄-PPy/GN catalysts showed excellent electrocatalytic performances for ORRs.

Ag nanoparticles were loaded on oxygen-doped carbonaceous polypyrrole nanotubes (OCPN) [76]. The Ag/OCPN catalysts possess comparable excellent activity with commercial Pt/C in alkaline solution. Moreover, the prepared catalysts showed superior stability and methanol tolerance.

3.3. Noble Metal Polypyrrole-Based Catalysts

In order to reduce the consumption of Pt material, Pt combined with other materials were widely investigated. Polypyrrole-based materials were widely used. Dendritic PtCo nanoclusters supported on sheet-like PPy (PtCo NCs/PPy) was proposed [77]. The synthesis method is a facile one-pot solvothermal method. Cetyltrimethylammonium chloride and pyrrole were applied as the capping agent and reductant, respectively. Meanwhile, under solvothermal conditions, the pyrrole was in situ polymerized to form PPy sheets. The prepared dendritic PtCo NCs/PPy showed an enlarged electrochemically active surface area (EASA, 30.95 m² g⁻¹). As compared with Pt₁Co₃ NPs, Pt₃Co₁ NPs, and commercial Pt/C catalysts, PtCo NCs/PPy showed the best catalytic performance and durability. The PPy sheets, as the supporting nitrogen-rich carbon materials, are essential in the material. Furthermore, PPy was used to modify mesoporous carbon black as the supporting material [78]. Ru-Pt NPs (1–2 nm) were dispersed on the PPy-modified carbon. In the process of PPy-modified carbon preparation, the amount of pyrrole was investigated. In order to test the ORR activities and the methanol tolerance of the material, the prepared electrocatalysts were tested according to both conventional electrochemical techniques and a direct methanol single cell. It is inspiring that the ORR performance of Ru-Pt/C-PP was far superior to that of Pt/C in the direct methanol fuel cell. The summary of electrocatalysts for ORR is shown in Tables 1 and 2.

Table 1. Summary of noble metal-free electrocatalysts for oxygen reduction reaction (ORR).

Electrocatalyst	Medium	Catalysts Loading [mg cm ⁻²]	Rotation Speed/rpm	Onset Potential/V vs. RHE	Halfwave Potential/V vs. RHE	Ref.
PANI-FeCo-C	0.5 M H ₂ SO ₄		900	0.93	0.79	[46]
3.0 Fe-PANI-L	0.5 M H ₂ SO ₄	0.6	1000	0.905	-	[48]
C-2PANI/PBA	0.5 M H ₂ SO ₄	0.36	1600	0.81	0.71	[49]
FeN _x C/C-F	0.1 M HClO ₄	0.8	1600	0.88	0.76	[51]
N/C/Fe-c	0.5 M H ₂ SO ₄	0.48	900	0.78	0.65	[52]
Fe/N-Cs-900	0.5 M H ₂ SO ₄	-	1600	0.845	0.717	[70]
(Co-PPy-TsOH/ C)P-A-P	0.5 M H ₂ SO ₄		900	0.78	0.71	[71]
CPANI/Mn ₂ O ₃	0.1 M KOH	0.28	1600	0.83	0.68	[53]
Fe-Co-N-C	0.1 M KOH	0.635	800	0.85	0.78	[68]
0.1-Fe-N-C ANFs	0.1 M KOH	-	1600	0.83	0.74	[69]
mNC-Fe ₃ O ₄ @rGO-2	0.1 M KOH	0.24	1600	0.96	0.83	[73]

Table 2. Summary of metal-free electrocatalysts for ORR.

Electrocatalyst	Medium	Catalysts Loading [mg cm ⁻²]	Rotation Speed/rpm	Onset Potential/V vs. RHE	Halfwave Potential/V vs. RHE	Ref.
NCNT-700	1 M NaOH	0.4	1600	0.88 at RRDE	0.8 V at RRDE	[33]
NCNTs-900	0.1 M KOH	0.64	1600	0.96	0.82	[34]
MEP-NC850	0.1 M KOH	0.25	1600	0.94	0.82	[37]
CNTs@PPy-P800	0.1 M KOH	0.2	1600	0.92	0.81	[59]
N,P-MC	0.1 M KOH	0.2	1600	0.93	0.84	[63]
NCNFs-900	0.1 M KOH		1600	0.92	0.82	[64]
NC-900	0.1 M KOH		1600	0.93	0.84	[65]

4. Summary and Perspective

Polymer-modified electrocatalysts are very promising materials for ORR. Polymers contain nitrogen atoms, which represented by PANI and PPy have been studied thoroughly. PANI or PPy alone or combined with carbon-based materials (nanoparticles, nanotubes, graphene, etc.) are pyrolyzed to generate N-doped carbon. Furthermore, different metals such as platinum, iron, cobalt, manganese, nickel, etc. are used to modify the N-doped carbon. As Table 1 shows, when binary metals are combined, such as Fe combined with Co, better ORR performance is achieved than when using single Fe or Co alone.

The ORR activities under different element additions are very interesting. Different elements, such as S, B, P, Fe, Co, Ni, Pd, Pt, etc., can be added to the catalysts. When, how, and how many of the elements are added to the catalysts are very important. When more than one metal element is added, normally we get several kinds of alloy nanoparticles, which are the important active sites. In a word, the additional elements matter in ORR catalysts.

For ORR catalysts, the pore area and size are very important. Having a pore size from 0.5 to 200 nm is very important in ORR activities. Further researches are needed to identify the best pore size. The phenomenon indicates that the polymers-derived materials should pay more attention to the pore structure and size.

In order to understand the active sites of the ORR catalysts, especially the nitrogen active sites, nitrogen-containing polymers could be designed for this purpose. Because there are many types of polymers with different nitrogen structure, they can be used as precursors of the catalysts. Furthermore, there are different morphologies of polymers, such as nanospheres, nanorods, microspheres, fibers, 3D structure gel, etc. These structures are interesting as precursors, and the relationship between activities and morphologies requires further research.

Funding: This research was funded by Shandong Natural Science Foundation (No. ZR2017QB009 and ZR2018MB036).

Conflicts of Interest: The authors declare no conflict of interest.

References

- Chen, H.C.; Song, Z.; Zhao, X.; Zhang, T.; Pei, P.C.; Liang, C. A review of durability test protocols of the proton exchange membrane fuel cells for vehicle. *Appl. Energy* **2018**, *224*, 289–299. [[CrossRef](#)]
- Wang, G.J.; Yu, Y.; Liu, H.; Gong, C.L.; Wen, S.; Wang, X.H.; Tu, Z.K. Progress on design and development of polymer electrolyte membrane fuel cell systems for vehicle applications: A review. *Fuel Process. Technol.* **2018**, *179*, 203–228. [[CrossRef](#)]
- Priya, K.; Sathishkumar, K.; Rajasekar, N. A comprehensive review on parameter estimation techniques for Proton Exchange Membrane fuel cell modelling. *Renew. Sustain. Energy Rev.* **2018**, *93*, 121–144. [[CrossRef](#)]
- Zhou, X.; Qiao, J.; Yang, L.; Zhang, J. A Review of Graphene-Based Nanostructural Materials for Both Catalyst Supports and Metal-Free Catalysts in PEM Fuel Cell Oxygen Reduction Reactions. *Adv. Energy Mater.* **2014**, *4*. [[CrossRef](#)]

5. Klingele, M.; Van Pham, C.; Fischer, A.; Thiele, S. A Review on Metal-Free Doped Carbon Materials Used as Oxygen Reduction Catalysts in Solid Electrolyte Proton Exchange Fuel Cells. *Fuel Cells* **2016**, *16*, 522–529. [[CrossRef](#)]
6. Banham, D.; Ye, S.; Pei, K.; Ozaki, J.-I.; Kishimoto, T.; Imashiro, Y. A review of the stability and durability of non-precious metal catalysts for the oxygen reduction reaction in proton exchange membrane fuel cells. *J. Power Sources* **2015**, *285*, 334–348. [[CrossRef](#)]
7. Zhang, C.L.; Shen, X.C.; Pan, Y.B.; Peng, Z.M. A review of Pt-based electrocatalysts for oxygen reduction reaction. *Front. Energy* **2017**, *11*, 268–285. [[CrossRef](#)]
8. Lafforgue, C.; Zadick, A.; Dubau, L.; Maillard, F.; Chatenet, M. Selected Review of the Degradation of Pt and Pd-based Carbon-supported Electrocatalysts for Alkaline Fuel Cells: Towards Mechanisms of Degradation. *Fuel Cells* **2018**, *18*, 229–238. [[CrossRef](#)]
9. Sui, S.; Wang, X.Y.; Zhou, X.T.; Su, Y.H.; Riffatc, S.; Liu, C.J. A comprehensive review of Pt electrocatalysts for the oxygen reduction reaction: Nanostructure, activity, mechanism and carbon support in PEM fuel cells. *J. Mater. Chem. A* **2017**, *5*, 1808–1825. [[CrossRef](#)]
10. Zhang, B.W.; Yang, H.L.; Wang, Y.X.; Dou, S.X.; Liu, H.K. A Comprehensive Review on Controlling Surface Composition of Pt-Based Bimetallic Electrocatalysts. *Adv. Energy Mater.* **2018**, *8*. [[CrossRef](#)]
11. Asset, T.; Chattot, R.; Fontana, M.; Mercier-Guyon, B.; Job, N.; Dubau, L.; Maillard, F. A Review on Recent Developments and Prospects for the Oxygen Reduction Reaction on Hollow Pt-alloy Nanoparticles. *Chemphyschem* **2018**, *19*, 1552–1567. [[CrossRef](#)] [[PubMed](#)]
12. Gomez-Marín, A.M.; Ticianelli, E.A. A reviewed vision of the oxygen reduction reaction mechanism on Pt-based catalysts. *Curr. Opin. Electrochem.* **2018**, *9*, 129–136. [[CrossRef](#)]
13. Antolini, E. The oxygen reduction on Pt-Ni and Pt-Ni-M catalysts for low-temperature acidic fuel cells: A review. *Int. J. Energy Res.* **2018**, *42*, 3747–3769. [[CrossRef](#)]
14. Gong, K.; Du, F.; Xia, Z.; Durstock, M.; Dai, L. Nitrogen-Doped Carbon Nanotube Arrays with High Electrocatalytic Activity for Oxygen Reduction. *Science* **2009**, *323*, 760–764. [[CrossRef](#)]
15. Guo, D.; Shibuya, R.; Akiba, C.; Saji, S.; Kondo, T.; Nakamura, J. Active sites of nitrogen-doped carbon materials for oxygen reduction reaction clarified using model catalysts. *Science* **2016**, *351*, 361–365. [[CrossRef](#)] [[PubMed](#)]
16. Chung, H.T.; Cullen, D.A.; Higgins, D.; Sneed, B.T.; Holby, E.F.; More, K.L.; Zelenay, P. Direct atomic-level insight into the active sites of a high-performance PGM-free ORR catalyst. *Science* **2017**, *357*, 479–483. [[CrossRef](#)] [[PubMed](#)]
17. Liu, T.; Zhao, P.; Hua, X.; Luo, W.; Chen, S.; Cheng, G. An Fe-N-C hybrid electrocatalyst derived from a bimetal-organic framework for efficient oxygen reduction. *J. Mater. Chem. A* **2016**, *4*, 11357–11364. [[CrossRef](#)]
18. Zhang, R.; He, S.; Lu, Y.; Chen, W. Fe, Co, N-functionalized carbon nanotubes in situ grown on 3D porous N-doped carbon foams as a noble metal-free catalyst for oxygen reduction. *J. Mater. Chem. A* **2015**, *3*, 3559–3567. [[CrossRef](#)]
19. Yang, F.; Zhao, P.; Hua, X.; Luo, W.; Cheng, G.; Xing, W.; Chen, S. A cobalt-based hybrid electrocatalyst derived from a carbon nanotube inserted metal-organic framework for efficient water-splitting. *J. Mater. Chem. A* **2016**, *4*, 16057–16063. [[CrossRef](#)]
20. Bu, L.; Zhang, N.; Guo, S.; Zhang, X.; Li, J.; Yao, J.; Wu, T.; Lu, G.; Ma, J.-Y.; Su, D.; et al. Biaxially strained PtPb/Pt core/shell nanoplate boosts oxygen reduction catalysis. *Science* **2016**, *354*, 1410–1414. [[CrossRef](#)]
21. Li, M.; Zhao, Z.; Cheng, T.; Fortunelli, A.; Chen, C.-Y.; Yu, R.; Zhang, Q.; Gu, L.; Merinov, B.V.; Lin, Z.; et al. Ultrafine jagged platinum nanowires enable ultrahigh mass activity for the oxygen reduction reaction. *Science* **2016**, *354*, 1414–1419. [[CrossRef](#)] [[PubMed](#)]
22. Choi, C.H.; Chung, M.W.; Kwon, H.C.; Park, S.H.; Woo, S.I. B, N- and P, N-doped graphene as highly active catalysts for oxygen reduction reactions in acidic media. *J. Mater. Chem. A* **2013**, *1*, 3694–3699. [[CrossRef](#)]
23. Yang, S.; Zhi, L.; Tang, K.; Feng, X.; Maier, J.; Muellen, K. Efficient Synthesis of Heteroatom (N or S)-Doped Graphene Based on Ultrathin Graphene Oxide-Porous Silica Sheets for Oxygen Reduction Reactions. *Adv. Funct. Mater.* **2012**, *22*, 3634–3640. [[CrossRef](#)]
24. Meng, Y.; Voiry, D.; Goswami, A.; Zou, X.; Huang, X.; Chhowalla, M.; Liu, Z.; Asefa, T. N-, O-, and S-Tridoped Nanoporous Carbons as Selective Catalysts for Oxygen Reduction and Alcohol Oxidation Reactions. *J. Am. Chem. Soc.* **2014**, *136*, 13554–13557. [[CrossRef](#)] [[PubMed](#)]

25. Qu, K.; Zheng, Y.; Dai, S.; Qiao, S.Z. Graphene oxide-polydopamine derived N, S-codoped carbon nanosheets as superior bifunctional electrocatalysts for oxygen reduction and evolution. *Nano Energy* **2016**, *19*, 373–381. [[CrossRef](#)]
26. Zhao, Z.; Wang, S.; Liang, R.; Li, Z.; Shi, Z.; Chen, G. Graphene-wrapped chromium-MOF(MIL-101)/sulfur composite for performance improvement of high-rate rechargeable Li-S batteries. *J. Mater. Chem. A* **2014**, *2*, 13509–13512. [[CrossRef](#)]
27. Wang, M.-Q.; Yang, W.-H.; Wang, H.-H.; Chen, C.; Zhou, Z.-Y.; Sun, S.-G. Pyrolyzed Fe-N-C Composite as an Efficient Non-precious Metal Catalyst for Oxygen Reduction Reaction in Acidic Medium. *ACS Catal.* **2014**, *4*, 3928–3936. [[CrossRef](#)]
28. Jiang, W.-J.; Gu, L.; Li, L.; Zhang, Y.; Zhang, X.; Zhang, L.-J.; Wang, J.-Q.; Hu, J.-S.; Wei, Z.; Wan, L.-J. Understanding the High Activity of Fe-N-C Electrocatalysts in Oxygen Reduction: Fe/Fe₃C Nanoparticles Boost the Activity of Fe-N-x. *J. Am. Chem. Soc.* **2016**, *138*, 3570–3578. [[CrossRef](#)]
29. Lin, L.; Zhu, Q.; Xu, A.-W. Noble-Metal-Free Fe-N/C Catalyst for Highly Efficient Oxygen Reduction Reaction under Both Alkaline and Acidic Conditions. *J. Am. Chem. Soc.* **2014**, *136*, 11027–11033. [[CrossRef](#)]
30. Maity, S.; Chatterjee, A. Conductive polymer-based electro-conductive textile composites for electromagnetic interference shielding: A review. *J. Ind. Text.* **2018**, *47*, 2228–2252. [[CrossRef](#)]
31. Xie, L.; Zhu, Y.T. Tune the phase morphology to design conductive polymer composites: A review. *Polym. Compos.* **2018**, *39*, 2985–2996. [[CrossRef](#)]
32. Amoabeng, D.; Velankar, S.S. A Review of Conductive Polymer Composites Filled With Low Melting Point Metal Alloys. *Polym. Eng. Sci.* **2018**, *58*, 1010–1019. [[CrossRef](#)]
33. Deng, H.; Li, Q.; Liu, J.; Wang, F. Active sites for oxygen reduction reaction on nitrogen-doped carbon nanotubes derived from polyaniline. *Carbon* **2017**, *112*, 219–229. [[CrossRef](#)]
34. Xu, J.; Lu, S.; Zhou, H.; Chen, X.; Wang, Y.; Xiao, C.; Ding, S. A Highly Efficient Electrocatalyst Derived from Polyaniline@CNTs-SPS** for the Oxygen Reduction Reaction. *Chemelectrochem* **2018**, *5*, 195–200. [[CrossRef](#)]
35. Quilez-Bermejo, J.; Morallon, E.; Cazorla-Amoros, D. Oxygen-reduction catalysis of N-doped carbons prepared via heat treatment of polyaniline at over 1100 degrees C. *Chem. Commun.* **2018**, *54*, 4441–4444. [[CrossRef](#)] [[PubMed](#)]
36. Huang, X.; Yin, X.; Yu, X.; Tian, J.; Wu, W. Preparation of nitrogen-doped carbon materials based on polyaniline fiber and their oxygen reduction properties. *Colloid Surface A* **2018**, *539*, 163–170. [[CrossRef](#)]
37. Zhou, F.; Wang, G.; Huang, F.; Zhang, Y.; Pan, M. Polyaniline derived N- and O-enriched high surface area hierarchical porous carbons as an efficient metal-free electrocatalyst for oxygen reduction. *Electrochim. Acta* **2017**, *257*, 73–81. [[CrossRef](#)]
38. Xing, S.; Yu, X.; Wang, G.; Yu, Y.; Wang, Y.; Xing, Y. Confined polyaniline derived mesoporous carbon for oxygen reduction reaction. *Eur. Polym. J.* **2017**, *88*, 1–8. [[CrossRef](#)]
39. Zhang, Y.; Zhuang, X.; Su, Y.; Zhang, F.; Feng, X. Polyaniline nanosheet derived B/N co-doped carbon nanosheets as efficient metal-free catalysts for oxygen reduction reaction. *J. Mater. Chem. A* **2014**, *2*, 7742–7746. [[CrossRef](#)]
40. Jiang, H.L.; Zhu, Y.H.; Feng, Q.; Su, Y.H.; Yang, X.L.; Li, C.Z. Nitrogen and Phosphorus Dual-Doped Hierarchical Porous Carbon Foams as Efficient Metal-Free Electrocatalysts for Oxygen Reduction Reactions. *Chem.-Eur. J.* **2014**, *20*, 3106–3112. [[CrossRef](#)]
41. Quilez-Bermejo, J.; Gonzalez-Gaitan, C.; Morallon, E.; Cazorla-Amoros, D. Effect of carbonization conditions of polyaniline on its catalytic activity towards ORR. Some insights about the nature of the active sites. *Carbon* **2017**, *119*, 62–71. [[CrossRef](#)]
42. Wei, Q.L.; Zhang, G.X.; Yang, X.H.; Fu, Y.Q.; Yang, G.H.; Chen, N.; Chen, W.F.; Sun, S.H. Litchi-like porous Fe/N/C spheres with atomically dispersed FeN_x promoted by sulfur as highly efficient oxygen electrocatalysts for Zn-air batteries. *J. Mater. Chem. A* **2018**, *6*, 4605–4610. [[CrossRef](#)]
43. Chenitz, R.; Kramm, U.I.; Lefevre, M.; Glibin, V.; Zhang, G.X.; Sun, S.H.; Dodelet, J.P. A specific demetalation of Fe-N-4 catalytic sites in the micropores of NC_Ar + NH₃ is at the origin of the initial activity loss of the highly active Fe/N/C catalyst used for the reduction of oxygen in PEM fuel cells. *Energy Environ. Sci.* **2018**, *11*, 365–382. [[CrossRef](#)]
44. Zhang, G.X.; Wei, Q.L.; Yang, X.H.; Tavares, A.C.; Sun, S.H. RRDE experiments on noble-metal and noble-metal-free catalysts: Impact of loading on the activity and selectivity of oxygen reduction reaction in alkaline solution. *Appl. Catal. B-Environ.* **2017**, *206*, 115–126. [[CrossRef](#)]

45. Wei, Q.L.; Zhang, G.X.; Yang, X.H.; Chenitz, R.; Barham, D.; Yang, L.J.; Ye, S.Y.; Knights, S.; Sun, S.H. 3D Porous Fe/N/C Spherical Nanostructures As High-Performance Electrocatalysts for Oxygen Reduction in Both Alkaline and Acidic Media. *Acs Appl. Mater. Interfaces* **2017**, *9*, 36944–36954. [[CrossRef](#)] [[PubMed](#)]
46. Wu, G.; More, K.L.; Johnston, C.M.; Zelenay, P. High-Performance Electrocatalysts for Oxygen Reduction Derived from Polyaniline, Iron, and Cobalt. *Science* **2011**, *332*, 443–447. [[CrossRef](#)] [[PubMed](#)]
47. Jaouen, F.; Herranz, J.; Lefevre, M.; Dodelet, J.P.; Kramm, U.I.; Herrmann, I.; Bogdanoff, P.; Maruyama, J.; Nagaoka, T.; Garsuch, A.; et al. Cross-Laboratory Experimental Study of Non-Noble-Metal Electrocatalysts for the Oxygen Reduction Reaction. *ACS Appl. Mater. Interfaces* **2009**, *1*, 1623–1639. [[CrossRef](#)]
48. Hu, Y.; Zhao, X.; Huang, Y.; Li, Q.; Bjerrum, N.J.; Liu, C.; Xing, W. Synthesis of self-supported non-precious metal catalysts for oxygen reduction reaction with preserved nanostructures from the polyaniline nanofiber precursor. *J. Power Sources* **2013**, *225*, 129–136. [[CrossRef](#)]
49. Wang, X.; Zou, L.; Fu, H.; Xiong, Y.; Tao, Z.; Zheng, J.; Li, X. Noble Metal-Free Oxygen Reduction Reaction Catalysts Derived from Prussian Blue Nanocrystals Dispersed in Polyaniline. *ACS Appl. Mater. Interfaces* **2016**, *8*, 8436–8444. [[CrossRef](#)]
50. Shi, K.-M.; Cheng, X.; Jia, Z.-Y.; Guo, J.-W.; Wang, C.; Wang, J. Oxygen reduction reaction of Fe-Polyaniline/Carbon Nanotube and Pt/C catalysts in alkali media. *Int. J. Hydrog. Energy* **2016**, *41*, 16903–16912. [[CrossRef](#)]
51. Zhang, J.; He, D.; Su, H.; Chen, X.; Pan, M.; Mu, S. Porous polyaniline-derived Fe_Nx/C catalysts with high activity and stability towards oxygen reduction reaction using ferric chloride both as an oxidant and iron source. *J. Mater. Chem. A* **2014**, *2*, 1242–1246. [[CrossRef](#)]
52. Wang, G.; Jiang, K.; Xu, M.; Min, C.; Ma, B.; Yang, X. A high activity nitrogen-doped carbon catalyst for oxygen reduction reaction derived from polyaniline-iron coordination polymer. *J. Power Sources* **2014**, *266*, 222–225. [[CrossRef](#)]
53. Cao, S.; Han, N.; Han, J.; Hu, Y.; Fan, L.; Zhou, C.; Guo, R. Mesoporous Hybrid Shells of Carbonized Polyaniline/Mn₂O₃ as Non-Precious Efficient Oxygen Reduction Reaction Catalyst. *ACS Appl. Mater. Interfaces* **2016**, *8*, 6040–6050. [[CrossRef](#)] [[PubMed](#)]
54. Zhou, X.; Xu, Y.; Mei, X.; Du, N.; Jv, R.; Hu, Z.; Chen, S. Polyaniline/beta-MnO₂ nanocomposites as cathode electrocatalyst for oxygen reduction reaction in microbial fuel cells. *Chemosphere* **2018**, *198*, 482–491. [[CrossRef](#)]
55. Peng, S.; Jiang, H.; Zhang, Y.; Yang, L.; Wang, S.; Deng, W.; Tan, Y. Facile synthesis of cobalt and nitrogen co-doped graphene networks from polyaniline for oxygen reduction reaction in acidic solutions. *J. Mater. Chem. A* **2016**, *4*, 3678–3682. [[CrossRef](#)]
56. Deng, Z.; Yi, Q.; Zhang, Y.; Nie, H.; Li, G.; Yu, L.; Zhou, X. Carbon Paper-Supported NiCo/C-N Catalysts Synthesized by Directly Pyrolyzing NiCo-Doped Polyaniline for Oxygen Reduction Reaction. *Nano* **2018**, *13*. [[CrossRef](#)]
57. Zhang, L.; Liu, X.; Wang, Y.; Chen, G.; Xing, S. Dual Role of Polyaniline for Achieving Ag Dendrites and Enhancing Its Oxygen Reduction Reaction Catalytic Activity. *Chemistryselect* **2017**, *2*, 10300–10303. [[CrossRef](#)]
58. Ye, B.; Cheng, K.; Li, W.; Liu, J.; Zhang, J.; Mu, S. Polyaniline and Perfluorosulfonic Acid Co-Stabilized Metal Catalysts for Oxygen Reduction Reaction. *Langmuir* **2017**, *33*, 5353–5361. [[CrossRef](#)]
59. Luo, Y.; Estudillo-Wong, L.A.; Cavillo, L.; Granozzi, G.; Alonso-Vante, N. An easy and cheap chemical route using a MOF precursor to prepare Pd-Cu electrocatalyst for efficient energy conversion cathodes. *J. Catal.* **2016**, *338*, 135–142. [[CrossRef](#)]
60. Liu, Y.; Chen, N.; Wang, F.; Cai, Y.; Zhu, H. Pt-Co deposited on polyaniline-modified carbon for the electro-reduction of oxygen: The interaction between Pt-Co nanoparticles and polyaniline. *New J. Chem.* **2017**, *41*, 6585–6592. [[CrossRef](#)]
61. Kaewsai, D.; Hunsom, M. Comparative Study of the ORR Activity and Stability of Pt and PtM (M = Ni, Co, Cr, Pd) Supported on Polyaniline/Carbon Nanotubes in a PEM Fuel Cell. *Nanomaterials* **2018**, *8*, 299. [[CrossRef](#)] [[PubMed](#)]
62. An, H.; Zhang, R.; Li, Z.; Zhou, L.; Shao, M.; Wei, M. Highly efficient metal-free electrocatalysts toward oxygen reduction derived from carbon nanotubes@polypyrrole core-shell hybrids. *J. Mater. Chem. A* **2016**, *4*, 18008–18014. [[CrossRef](#)]

63. Zhang, Z.; Sun, J.; Dou, M.; Jo, J.; Wang, F. Nitrogen and Phosphorus Codoped Mesoporous Carbon Derived from Polypyrrole as Superior Metal-Free Electrocatalyst toward the Oxygen Reduction Reaction. *ACS Appl. Mater. Interfaces* **2017**, *9*, 16236–16242. [[CrossRef](#)] [[PubMed](#)]
64. Xia, W.; Qu, C.; Liang, Z.; Zhao, B.; Dai, S.; Qiu, B.; Jiao, Y.; Zhang, Q.; Huang, X.; Guo, W.; et al. High-Performance Energy Storage and Conversion Materials Derived from a Single Metal Organic Framework/Graphene Aerogel Composite. *Nano Lett.* **2017**, *17*, 2788–2795. [[CrossRef](#)] [[PubMed](#)]
65. Yang, M.; Liu, Y.; Chen, H.; Yang, D.; Li, H. Porous N-Doped Carbon Prepared from Triazine-Based Polypyrrole Network: A Highly Efficient Metal-Free Catalyst for Oxygen Reduction Reaction in Alkaline Electrolytes. *ACS Appl. Mater. Interfaces* **2016**, *8*, 28615–28623. [[CrossRef](#)] [[PubMed](#)]
66. Morozan, A.; Jegou, P.; Campidelli, S.; Palacin, S.; Josselme, B. Relationship between polypyrrole morphology and electrochemical activity towards oxygen reduction reaction. *Chem. Commun.* **2012**, *48*, 4627–4629. [[CrossRef](#)] [[PubMed](#)]
67. Osmieri, L.; Videla, A.H.A.M.; Specchia, S. Optimization of a Fe-N-C electrocatalyst supported on mesoporous carbon functionalized with polypyrrole for oxygen reduction reaction under both alkaline and acidic conditions. *Int. J. Hydrog. Energy* **2016**, *41*, 19610–19628. [[CrossRef](#)]
68. Osmieri, L.; Zafferoni, C.; Wang, L.; Videla, A.H.A.M.; Lavacchi, A.; Specchia, S. Polypyrrole-Derived Fe-Co-N-C Catalyst for the Oxygen Reduction Reaction: Performance in Alkaline Hydrogen and Ethanol Fuel Cells. *Chemelectrochem* **2018**, *5*, 1954–1965. [[CrossRef](#)]
69. Sun, M.; Wu, X.; Liu, C.; Xie, Z.; Deng, X.; Zhang, W.; Huang, Q.; Huang, B. The in situ grown of activated Fe-N-C nanofibers derived from polypyrrole on carbon paper and its electro-catalytic activity for oxygen reduction reaction. *J. Solid State Electrochem.* **2018**, *22*, 1217–1226. [[CrossRef](#)]
70. Sun, T.; Yang, M.; Chen, H.; Liu, Y.; Li, H. N-doped and N/Fe-codoped porous carbon spheres derived from tetrazine-based polypyrrole as efficient electrocatalysts for the oxygen reduction reaction. *Appl. Catal. A Gen.* **2018**, *559*, 102–111. [[CrossRef](#)]
71. Sha, H.-D.; Yuan, X.; Li, L.; Ma, Z.; Ma, Z.-F.; Zhang, L.; Zhang, J. Experimental identification of the active sites in pyrolyzed carbon-supported cobalt-polypyrrole-4-toluenesulfonic acid as electrocatalysts for oxygen reduction reaction. *J. Power Sources* **2014**, *255*, 76–84. [[CrossRef](#)]
72. Jia, X.; Gao, S.; Liu, T.; Li, D.; Tang, P.; Feng, Y. Fabrication and Bifunctional Electrocatalytic Performance of Ternary CoNiMn Layered Double Hydroxides/Polypyrrole/Reduced Graphene Oxide Composite for Oxygen Reduction and Evolution Reactions. *Electrochim. Acta* **2017**, *245*, 51–60. [[CrossRef](#)]
73. Zhu, S.Y.; Tian, H.; Wang, N.; Chen, B.; Mai, Y.Y.; Feng, X.L. Patterning Graphene Surfaces with Iron-Oxide-Embedded Mesoporous Polypyrrole and Derived N-Doped Carbon of Tunable Pore Size. *Small* **2018**, *14*. [[CrossRef](#)]
74. Ren, S.; Guo, Y.; Ma, S.; Mao, Q.; Wu, D.; Yang, Y.; Jing, H.; Song, X.; Hao, C. Co₃O₄ nanoparticles assembled on polypyrrole/graphene oxide for electrochemical reduction of oxygen in alkaline media. *Chin. J. Catal.* **2017**, *38*, 1281–1290. [[CrossRef](#)]
75. Ren, G.; Li, Y.; Guo, Z.; Xiao, G.; Zhu, Y.; Dai, L.; Jiang, L. A bio-inspired Co₃O₄-polypyrrole-graphene complex as an efficient oxygen reduction catalyst in one-step ball milling. *Nano Res.* **2015**, *8*, 3461–3471. [[CrossRef](#)]
76. Xiao, D.; Ma, J.; Chen, C.; Luo, Q.; Ma, J.; Zheng, L.; Zuo, X. Oxygen-doped carbonaceous polypyrrole nanotubes-supported Ag nanoparticle as electrocatalyst for oxygen reduction reaction in alkaline solution. *Mater. Res. Bull.* **2018**, *105*, 184–191. [[CrossRef](#)]
77. Chen, X.-L.; Zhang, L.; Feng, J.-J.; Wang, W.; Yuan, P.-X.; Han, D.-M.; Wang, A.-J. Facile solvothermal fabrication of polypyrrole sheets supported dendritic platinum-cobalt nanoclusters for highly efficient oxygen reduction and ethylene glycol oxidation. *J. Colloid Interface Sci.* **2018**, *530*, 394–402. [[CrossRef](#)]
78. Escudero Cid, R.; Gomez de la Fuente, J.L.; Rojas, S.; Garcia Fierro, J.L.; Ocon, P. Polypyrrole-Modified-Carbon-Supported Ru-Pt Nanoparticles as Highly Methanol-Tolerant Electrocatalysts for the Oxygen-Reduction Reaction. *Chemcatchem* **2013**, *5*, 3680–3689. [[CrossRef](#)]

